Local Stress Relaxation in a Ti-6A1-4V-2Fe/SCS-6 SiC Composite During Thermal Cycling

M. R. JAMES, W. L. MORRIS and B. N. COX
Rockwell International Science Center, Thousand Oaks, CA 91360, USA

ABSTRACT

Preliminary observations of the deformation near two fibers resulting from a single thermal cycle of a thin sheet metal matrix composite are presented. The in-plane and out-of-plane displacements at the fiber/matrix interface and in the matrix between two fibers exhibit a complex pattern resulting from the relaxation of residual stresses in the matrix. This relaxation is mediated by the coalescence of two radial interfiber cracks formed parallel to the composite surface during consolidation, by microcracking and sliding in the fiber coating and fiber/matrix interface, and by plastic flow in the matrix near the interface. The fiber, fiber coating, reaction zone and matrix all have distinct displacement movements which indicate lack of chemical bonding in the interfacial region. These interfacial microcracks extend in circumference during repeated thermal cycles, implying degradation of the mechanical integrity of the composite.

KEYWORDS

Metal-matrix composite; thermal fatigue; residual stress; interface cracks; deformation

EXPERIMENTAL PROCEDURE

The Ti-6Al-4V-2Fe alloy reinforced with continuous SCS-6 SiC fibers* has been described previously.[1] The composite was manufactured by consolidating three layers of SCS-6 fiber mat stacked alternately with four layers of 250 μm thick alloy foil. The 1.1 mm thick consolidated sheet was cross-sectioned normal to the fibers, polished and lightly etched to reveal the microstructure. The area shown in Fig. 1, located in the outer row of fibers, was chosen for analysis because it incorporates interfiber matrix cracks extending from each fiber that had not completely linked during processing. Such cracks occur frequently in the manufacture of high-temperature metal-matrix composites (MMCs) because of incomplete diffusion bonding between the matrix foils during consolidation or high tensile hoop stresses that develop around the fibers from the thermal expansion mismatch between fibers and matrix.[2]

* Textron Specialty Products, Lowell, Massachusetts

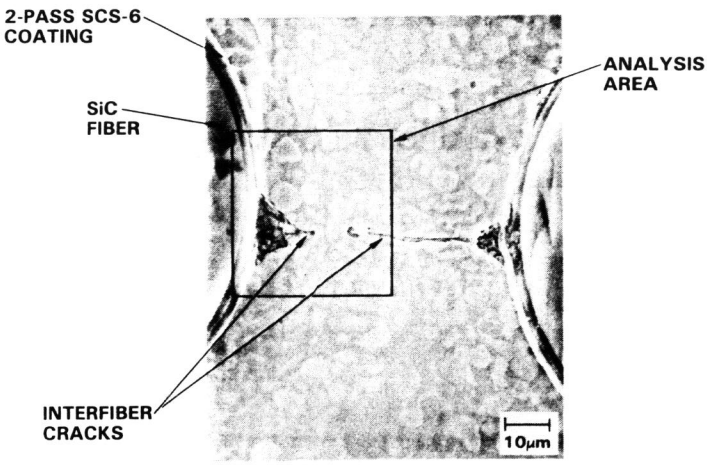

Fig. 1 Micrograph showing interfiber microcracks in as-polished section of Ti 6Al-4V-2Fe/SCS-6 composite.

Displacement fields generated by the application of one and five thermal cycles were measured by comparing 1000X SEM micrographs, taken before and after the sample was heated in air to 790°C and left to cool to room temperature. A schematic of the High Accuracy Strain Mapping (HASMAP) facility used to measure the surface displacements is shown in Fig. 2. The instrument was designed at the Science Center and its components integrated by TAU Corp.* It is described in detail in Ref. 3. Each pair of micrographs to be analyzed was placed on a precise X-Y table and passed in turn under a solid-state video camera. Corresponding windows of about 3 mm x 3 mm

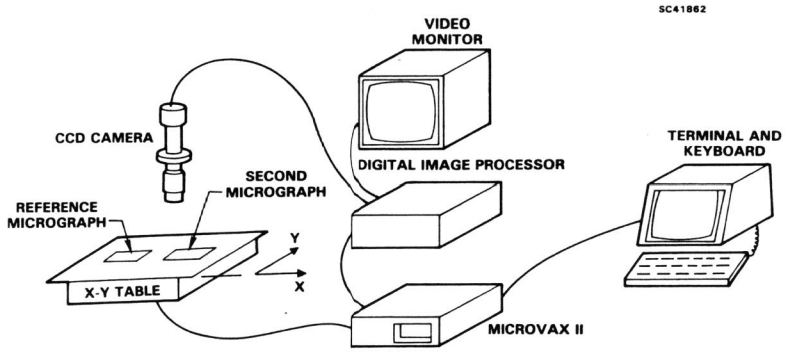

Fig. 2 Schematic of HASMAP.

* TAU Corp, Los Gatos, California

on each micrograph (3 μm x 3 μm on the sample) were digitized into 128 x 128 pixels with 256 levels of grey. The two stored images were then analyzed by a combination of cross correlation calculations using fast Fourier transforms[4] and error minimization procedures[3] to deduce the relative displacements between the local regions on the two micrographs. This procedure was carried out over an 8 x 8 array of windows to obtain a displacement map. Since the local intensities are nearly unchanged between micrographs, except for the small relative displacement being sought, the accuracy of this relative positioning measurement far exceeds the point-to-point resolution of the SEM.[5] However, because of oxidation on the heated sample and the low spatial contrast of the images analyzed, the displacement resolution in this work was only about 50 nm. With sufficient spatial frequency information and higher magnification, displacements have been measured to an accuracy of 2 nm by HASMAP.[3]

SEM micrographs were recorded at normal and oblique angles before and after thermal cycling (a set of four micrographs). These micrographs contain the data necessary to determine the differential in-plane and out-of-plane displacements for each pair of windows.[6] Separation of the displacements into in-plane and out-of-plane components was most easily accomplished if the windows were at the same (x,y) coordinates in the tilted and untilted micrographs. This was accomplished, accounting for the foreshortening in the tilted micrograph. While the data were taken over an essentially rectangular array, some windows were positioned to take advantage of sites of higher contrast in the image. Typical analysis time, including all setup, was approximately two hours.

Repeated comparison of the calculated displacement vector field to stereoscopic observations of the micrographs showed that HASMAP was resolving fine detail such as interfacial microcracking and matrix deformation that could only otherwise be defined with careful, time-consuming quantitative stereoscopy. However, a few relative displacements calculated by HASMAP were in substantial error. With these, the cross-correlation routine was finding the wrong correlation peak because of the lack of detail within the 128 x 128 pixel array being analyzed. This occurred most frequently on the SiC region of the fiber where little fine image structure existed. These errors were typically five times greater than the surrounding displacements and so were easily identified. For these locations, the displacements were set either to a value obtained by stereoscopy[5] when the errors occurred in the fiber or, for the few times errors were obtained in the matrix, to the average of the results from neighboring points.

To display the displacements, a synthetic image of the analyzed area was created by digitizing 16 fields of view (each field 512 x 480 pixels) covering roughly 50 mm square on the micrograph, compressing the fields by averaging the value of cells of 4 x 4 pixels, assigning the average intensity to one pixel in a 128 x 120 pixel field and butting the fields together to form a single 512 x 480 pixel montage. The central locations of the 64 windows on this synthetic digital image were calculated and the corresponding displacement vectors were displayed at each location. Image processing capabilities were used to overlay grid lines and distort the synthetic image according to the magnitude of the local displacement to create two- and three-dimensional representations of the displacements.

RESULTS

One thermal cycle to 790°C and back to room temperature caused the interfiber cracks to grow towards each other and the interface to partially crack, as illustrated in Fig. 3. After five cycles, the interfiber cracks had coalesced and the interfacial cracks had completely encompassed the fiber. Displacements observed in the matrix are consistent with partial relaxation of the tensile longitudinal and circumferential residual stresses formed in the matrix when the composite cooled after consolidation.

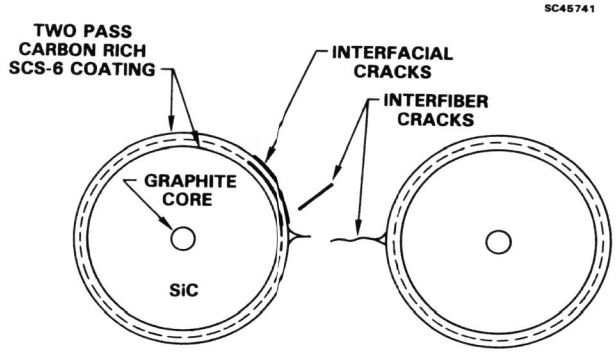

Fig. 3 Illustration of interfiber and interfacial cracks found after one thermal cycle.

Out-of-Plane Displacements

Only the two interfiber cracks are visible in individual micrographs taken of the polished and etched surface before thermal cycling (Fig. 1). Comparison by HASMAP of pairs of micrographs taken before and after one thermal cycle reveals additional cracks as illustrated in Fig. 3. Displacements measured on the tilted micrographs are shown in Fig. 4. Although the vectors are a combination of the in-plane and out-of-plane displacements, the latter are significantly larger than the former. The interface crack is apparent in Fig. 5a where the out-of-plane displacements have been used to

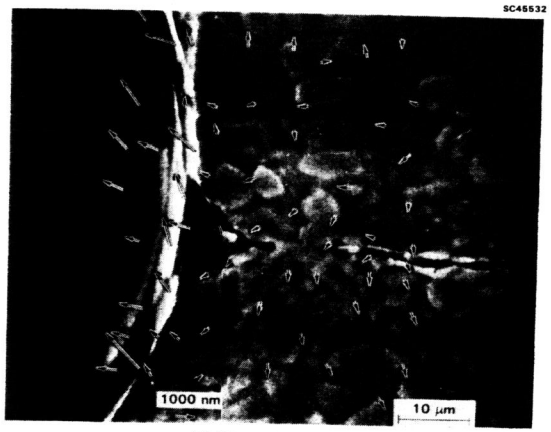

Fig. 4 Displacement vectors overlayed onto montage of analyzed area. Each vector begins at the central location of the measurement window. The lower left vector gives the scale of the displacement vectors and the lower right bar gives the scale of the digital micrograph, both in specimen dimensions.

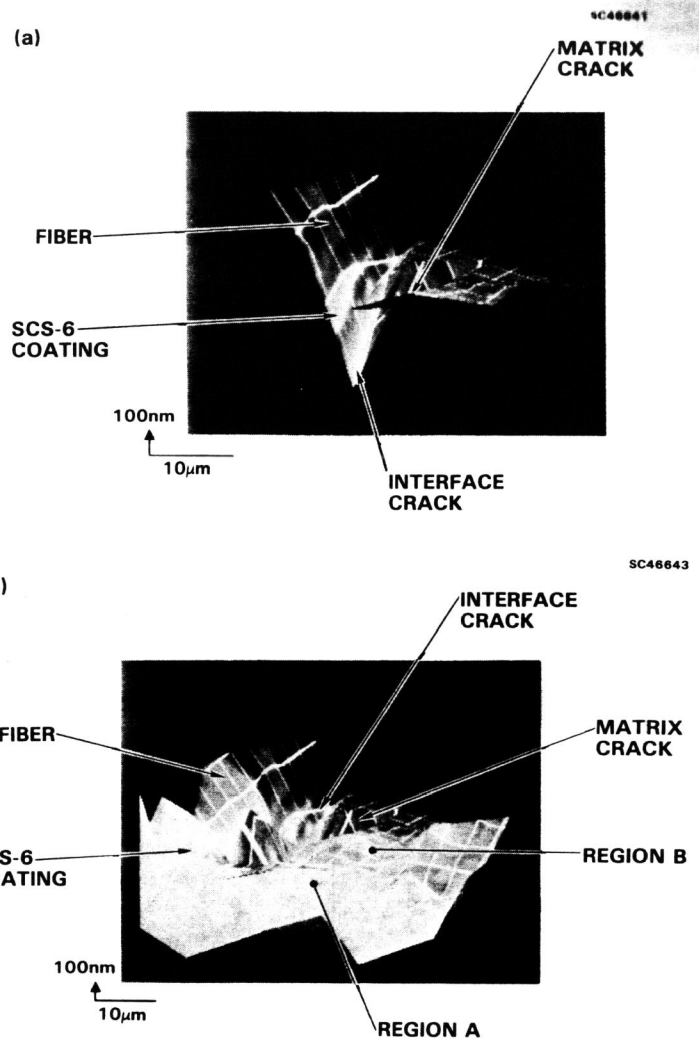

Fig. 5 Perspective view where out-of-plane displacements have been used to modulate the surface height. (a) Sectional view highlighting sharp changes in displacement by interface crack and matrix crack; (b) full view. Horizontal bar is scale of undistorted micrograph and vertical vector is out-of-plane displacement scale, in specimen dimensions.

modulate the image. The perspective in Fig. 5a has been sectioned parallel to the interfiber crack plane to reveal better the cracks in the interface and matrix. In the full view of the analyzed area (Fig. 5b), these are partially hidden by the foreground. The grid spacing for displacement analysis was not chosen to be dense enough to resolve the fine displacement structure of the various layers in the SCS coating, but a schematic view of the displacements across the interface obtained with the help of additional stereoscopic analysis is presented in Fig. 6. The discontinuous relative heights of the layers in the SCS coating show the complex microscopic deformation that took place to accommodate the mismatch of thermal strains between the fiber and matrix. The SCS layers on the SiC fiber were deposited from chemical vapor in two passes, leaving distinct interfaces that can be seen in Fig. 1. One interfacial crack divided the SCS coating into debonded inner and outer layers. Another interfacial crack formed between the outer layer and the matrix. The outer SCS layer displayed a significant drop in height from both the fiber and matrix over each thermal cycle.

The out-of-plane displacements in the matrix (Fig. 5b) show that the entire matrix has dropped around the fiber, probably due to relaxation of the residual tensile stress in the matrix in the longitudinal (fiber) direction. The displacement is larger on one side of the plane of the interfiber cracks (Fig 5b, region A) because a crack formed at the adjacent fiber interface. On the side B of the interfiber cracks, the matrix and fiber are still clearly attached after one thermal cycle. The withdrawal of the matrix in region B is apparently mediated by plastic flow. X-ray measurements of the average longitudinal residual stress in the matrix confirm that it is tensile and can easily exceed half the yield strength of the matrix at room temperature.[7] Near the interfaces, the local stresses will be even higher. Thus, some plastic deformation on the freshly cut and polished surface can be anticipated.

SC45742

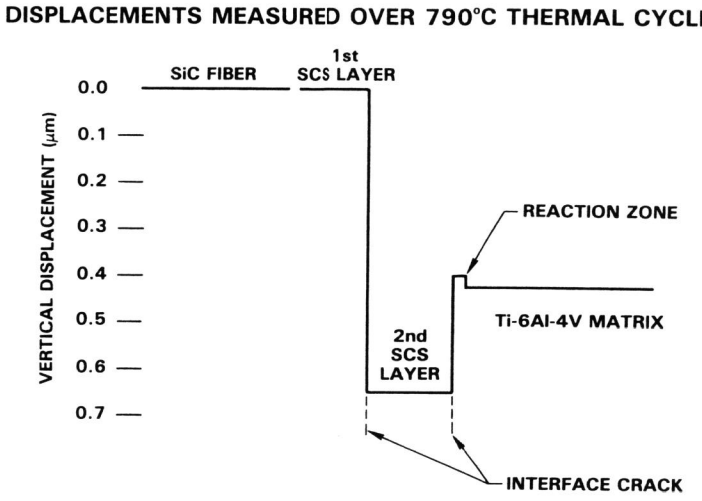

Fig. 6 Illustration of the out-of-plane displacements showing different movements of the fiber, the SCS layers, and the matrix. This cross section was taken approximately at the front edge of Fig. 5a.

In-Plane Displacements

To view the in-plane displacements, a square grid was written onto the digital image and deformed according to the measured displacements. Stretching of the square over a thermal cycle indicates tensile movement in the direction of the stretch, while shrinkage indicates a compressive residual strain. The square distorts to a parallelogram under shear. Figure 7 shows that over the first thermal cycle the matrix near the interface experienced compressive movement in the hoop direction and tensile movement in the radial direction. These displacements relax the tensile hoop and compressive radial residual stresses formed during manufacture (see Discussion). The displacements near the interfiber crack plane indicate a mixed mode residual opening of the crack, with a tensile Mode I component.

SC45533

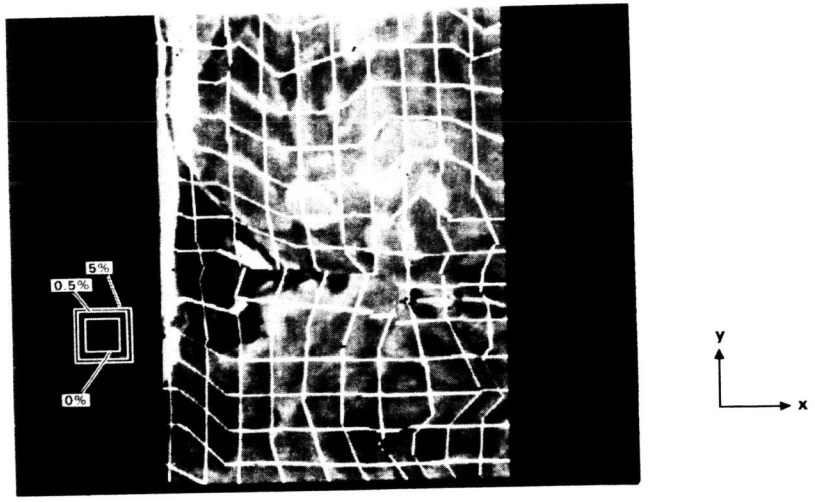

Fig. 7 Square grid distorted by the in-plane displacements superimposed onto the analyzed area. The squares to the left of the image show the original grid size, and 0.5% and 5.0% deformations on a log scale. A log scale was used to accentuate the small matrix deformation in the presence of the large displacements at the crack edges.

After five thermal cycles, the radial interfiber cracks had extended completely across the matrix and had coalesced. They had also linked up with the interface cracks, which had grown completely around the fiber. The interfiber cracks were always easily visible in individual micrographs. The two interface cracks on either side of the outer SCS layer were less easily identified, but by five thermal cycles could be discerned without the use of displacement analysis.

DISCUSSION

Thermal expansion mismatch between fibers and matrix causes large, triaxial residual stresses to arise during cooldown of the MMCs following the last stage of processing. The impact of these highly inhomogeneous stresses and their stability during service are not well understood. This paper presents a first attempt to use high resolution surface displacement measurements to reveal how the residual stresses and the state of microcracking evolve during thermal cycling.

In the region of the composite depicted in Fig. 1, the residual stresses may be expected from elastic analysis[8] to be qualitatively as follows. The matrix, which has the greater coefficient of thermal expansion, will bear tensile stresses σ_ℓ in the longitudinal direction (parallel to the fiber axes) and σ_θ in the circumferential direction around each fiber. The component σ_r in the radial direction around each fiber will depend strongly on location and fiber separation, being compressive at points near the line between the centers of two closely spaced fibers and tensile where one of those fibers abuts a large interstitial region of the matrix.[8] The corresponding stresses σ_ℓ', σ_θ' and σ_r' in the fibers will all be compressive, except that σ_r' approaching the interface must equal σ_r there. All of these stresses will be modified by the presence of the free surface upon which observations were made, but their general disposition remains as just described. The most important surface effect is that the stresses at the intersection of the surface and the various interfaces may be singular.[9] Such irregularities will be relieved by plastic deformation or interfacial debonding and sliding. One would expect this relief and some relief of residual stresses elsewhere near the surface to occur when the specimen is cut at room temperature.

Upon subsequent heating, the residual stresses presumably diminish in magnitude, since they were initially zero at the elevated temperature of the final stage of processing. One consequence of the reduction of residual stresses is that, in regions of the interface where σ_r and σ_r' are compressive, the interface becomes less tightly pressed together. Now the SCS coating has been shown by TEM examination to contain turbostratic carbon layers in which the basal planes are oriented normal to the radial direction of the fibers.[10] Such layers may be weakly bonded and ideal locations for slip with frictional resistance. Presuming Coulomb friction, the reduction of compressive stresses σ_r and σ_r' would therefore facilitate slip in the longitudinal direction between fibers and matrix. The sense of the slip is such as to relieve the large longitudinal residual stresses in matrix and fibers - the matrix sinks into the composite - and this must be the direction of the hysteresis revealed by differential displacement measurements. This is one mechanism that can account for the discontinuity visible in the SCS coating in Figs. 4, 5 and 6. Note, however, that since no hysteresis was visible in another experiment over one heating to just 490°C, it can be inferred that the compressive radial stresses are not low enough to permit frictional sliding until temperatures higher than this are achieved. For this reason, room-temperature measurements of longitudinal strength and stiffness can be nonconservative indicators of interfacial damage.

Although the residual stresses fall with heating, so too does the flow stress in the matrix, and the residual stresses may therefore cause plastic flow at elevated temperatures. This has not happened on heating to 490°C as noted above, but plastic flow has clearly contributed to the hysteresis visible in Fig. 5 near the unfailed interface in region B. The stresses in that region must also have been enhanced at elevated temperatures by the slipping of the interfaces on the other side of the interfiber cracks.

The existence of numerous interfiber cracks in high-temperature MMC's has driven researchers towards developing alternative manufacturing techniques as well as new fibers with better thermal expansion match to the matrix. Much more subtle defects such as interfacial microcracks need also to be understood before these composites will perform adequately in severe thermomechanical environments. The 790°C thermal cycle over which the measurements presented here were made is admittedly quite severe, but similar, slower damage will accrue over temperature cycles expected in service. The rate of damage can be studied most sensitively using surface displacement measurements, which identify microcrack formation much sooner than changes are found in bulk properties. The ability of HASMAP to sense microscopic damage will provide a rational data base for discerning improvements in material integrity as processing and materials strategies change. Surface displacement analysis is an accurate and quantitative technique for investigating these microscopic phenomena. The use of digital image correlation has both improved the accuracy and increased the speed of measurement significantly. It also provides opportunity for a wide range of researchers to carry out such investigations since the technique can be automated to a high degree. Measurements can be made on very small specimens without having to produce samples large enough for traditional fatigue testing.

ACKNOWLEDGEMENTS

The Ti-6Al-4V-2Fe/SCS-6 composite was kindly supplied by Cecil Rhodes. The research was funded by Rockwell International IR&D.

REFERENCES

1. Rhodes, C. and R.A Spurling (1988). " SiC Reinforced Ti-6Al-4V-2Fe," submitted to Metal. Trans. A.
2. Ghosh, A.K., "Processing of Metal-Matrix Composites (1988). Proc. of ONR Workshop on Materials Processing, Hyderbad, India, January, in print.
3. James, M.R., W.L. Morris and B.N. Cox (1988). "Surface Displacement Measurements by Digital Image Correlation," submitted to Exp. Mechanics.
4. Mostafavi, H. and F.W. Smith (1978). "Image Correlation With Geometric Distortion," IEEE Trans. on Aerospace and Electronic Systems, AES-14, 487-500.
5. Cox, B.N., W.L. Morris and M.R. James (Aug. 1986). "High Sensitivity, High Spatial Resolution Strain Measurements in Composites and Alloys," Proc. Nondestructive Testing and Evaluation of Advanced Materials and Composites, Colorado Springs, 25-39.
6. Morris, W.L., R.V. Inman and B.N. Cox (1988). "Microscopic Deformation in a Heated Unidirectional Graphite/Epoxy Composite," J. Materials Science, in press.
7. James, M.R. and B.N. Cox (1988). "Residual Stress Measurements in High Temperature Metal Matrix Composites," submitted to Metal. Trans. A.
8. Asamoah, N.K. and W.G. Wood (1970). "Thermal Self-Straining of Fiber-Reinforced Materials," J. Strain Analysis 5, 88-97.
9. Bogy, D.B. (1975). "The Plane Solution for Joined Dissimilar Elastic Semistrips Under Tension," J. Appl. Mech. 42, 93-8.
10. Pirouz, P. (1988). "Microstructure of Composite Interface and Its Relation to Interfacial Strength," Proc. Surface and Interfaces of Ceramic Materials, ed., L.C. Dufour and C. Monty, Oleron, France, Sept. 4-16.